Supplementary Materials

Structures and phase transitions in the neat 4,4'-di-*tert*-butyl-2,2'-bipyridyl and in its molecular complexes with either brom- or iodanilic acid

Magdalena Rok[a]*, Przemysław Szklarz[a], Marcin Moskwa[a], Monika Kijewska[a], Jan Baran[b], Grażyna Bator[a], Wojciech Medycki[c], Michaela Zamponi[d]

a Faculty of Chemistry, University of Wroclaw, 14 F. Joliot – Curie, 50-383 Wroclaw, Poland

b Institute of Low Temperature and Structure Research, Polish Academy of Science, Okólna 2, PO Box 937, 50-950 Wroclaw, Poland

c Institute of Molecular Physics, Polish Academy of Sciences, Smoluchowskiego 17, 60-179 Poznań, Poland

d Jülich Centre for Neutron Science (JCNS) at Heinz Maier-Leibnitz Zentrum (MLZ), Forschungszentrum Jülich GmbH, Lichtenbergstr. 1, 85748 Garching, Germany

*e-mail: magdalena.rok@chem.uni.wroc.pl

CAPTIONS OF FIGURES

Fig. 1S. Simultaneous curves of thermogravimetric analysis and differential thermal analysis (2 K min ^{1}) (a) pure **dtBBP**; (b) **dtBBP·CLA**; (c) **dtBBP·BRA**; (d) **dtBBP·IA**.

Fig. 2S. DSC curves for the (a) pure **dtBBP** and (b) **dtBBP·IA** crystals. Arrows show directions of runs (cooling or heating).

Fig. 3S. The supramolecular chain of the **dtBBP·BRA** complex (155 K) formed by N-H···(O, O) and O-H···(N, O) bifurcated hydrogen bonds (dashed lines). Atoms labelled with suffixes (#2) are at positions x, $1+y$, z.

Fig. 4S. The interactions of the π-π stacking type in the crystal structure of the **dtBBP·BRA** complex at 155 K, the projection along ***b***-axis.

Fig. 5S. The ···dtBBP-IA-dtBBP-IA··· chain along the ***b***-axis.

Fig. 6S. The layers and stacks of molecules in the structure of dtBBP·IA with the directions of the chains indicated (phase II).

Fig. 7S. The frequency dependence of (a) the real part, ε': and (b) the imaginary part, ε"; of the permittivity at several temperatures measured for **dtBBP·BRA**

Fig. 8S. The dependence of ε" *versus* ε' for the single crystal of the **dtBBP·BRA** complex. The solid line represents fit to the Cole-Cole equation (Eq. (1)).

Fig. 9S. Raman and IR spectra of the a) pure-**dtBBP** and b) **dtBBP·IA**

Fig. 10S. Temperature dependence of the average value lnΓ versus 1000/T for the pure **dtBBP** base (violet-circle), **dtBBP·CLA** (blue-triangle), **dtBBP·BRA** (yellow-square) and **dtBBP·IA** (green-diamond).

Fig. 11S. The temperature dependence of the spin–lattice relaxation time (T_1) for all complexes in the range between 8 and 100K a) pure-**dtBBP**, b) **dtBBP·CLA**, c) **dtBBP·BRA**, d) **dtBBP·IA**. The figures c, d, e and f were drawn for the temperature range between 100 and 50K.

Fig. 12S. Temperature dependence of the real part of the complex electric permittivity for the as-grown **dtBBP·IA** single crystal.

Fig. 13S. Temperature dependence of the imaginary part of the complex electric permittivity for the as-grown **dtBBP·IA** single crystal

CAPTIONS OF TABLES

Table 1S. Geometrical parameters (length and angle) and energies of the hydrogen bonds.

Table 2S. Crystal data and structure refinement for pure **dtBBP** and its complexes.

Table 3S. Selected bond lengths [Å] and angles [º] for **dtBBP** at 130 **(III)**, 190 **(II)** and 250 K **(I)**.

Table 4S. Selected bond lengths [Å] and angles [º] for **dtBBP·CLA** at 295[1], for **dtBBP·BRA** at 155 K and for **dtBBP·IA** at 295**(II)**, 345 K **(I)**.

Table 5S. Hydrogen bonds in the crystalline state of **dtBBP·CLA** [Å,º].

Table 6S. Hydrogen bonds in the crystalline state of **dtBBP·BRA** [Å,º].

Table 7S. Hydrogen bonds in the crystalline state of **dtBBP·IA** at 345K **(I)** and 295K **(II)** [Å,º].

Table 8S. Wavenumber (cm^{-1}), intensity and tentative assignments of the bands observed in the IR and Rama spectra of **dtBBP** at 11 and 300 K.

Table 9S. Wavenumber (cm^{-1}), intensity and tentative assignments of the bands observed in the IR and Raman spectra of **dtBBP·IA** at 303 **(II)** and 353 K **(I)**.

Table 10S. Parameters, E_a, τ_0, C obtained from ^{1}H-NMR interaction.

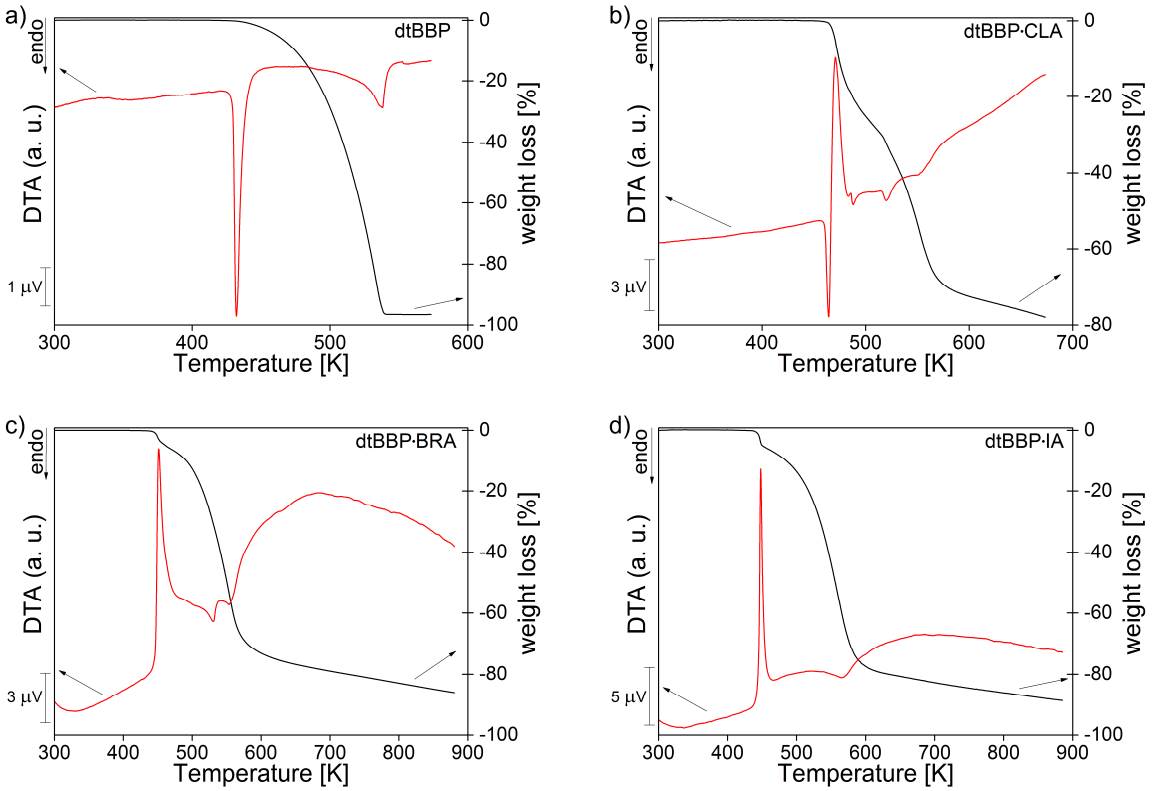

Fig. 1S. Simultaneous curves of thermogravimetric analysis and differential thermal analysis (2 K min ^{1}) (a) pure **dtBBP**; (b) **dtBBP·CLA**; (c) **dtBBP·BRA**; (d) **dtBBP·IA**.

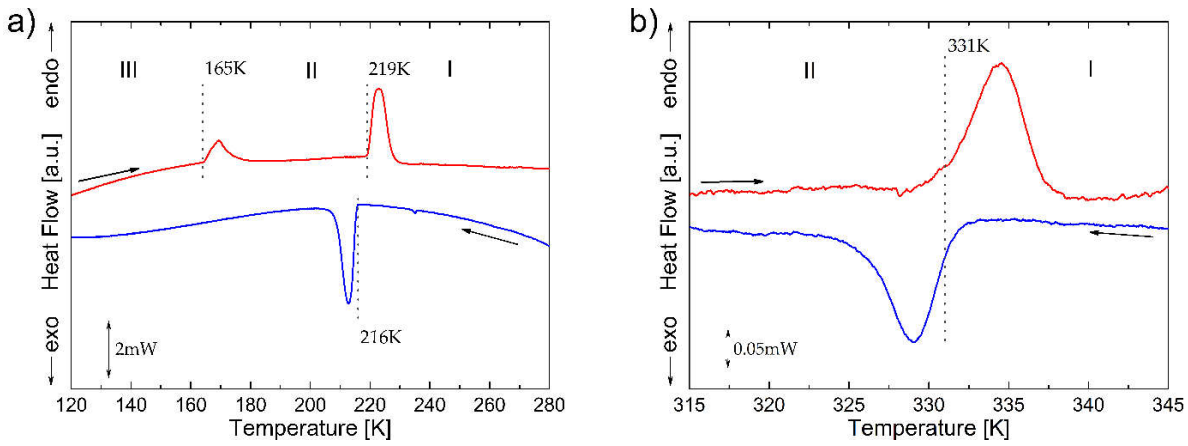

Fig. 2S. DSC curves for the (a) pure **dtBBP** and (b) **dtBBP·IA** crystals. Arrows show directions of runs (cooling or heating).

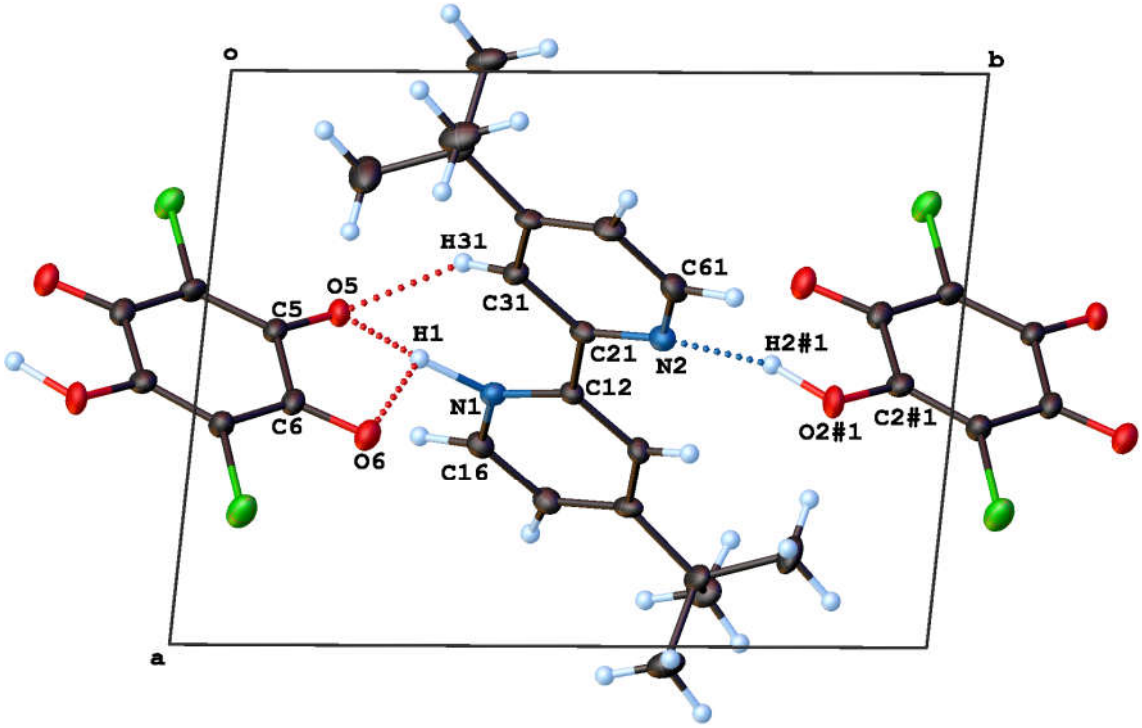

Fig. 3S. The supramolecular chain of the **dtBBP·BRA** complex (155 K) formed by N-H···(O, O) and O-H··· (N, O) bifurcated hydrogen bonds (dashed lines). Atoms labelled with suffixes (#2) are at positions *x*, 1+*y*, *z*.

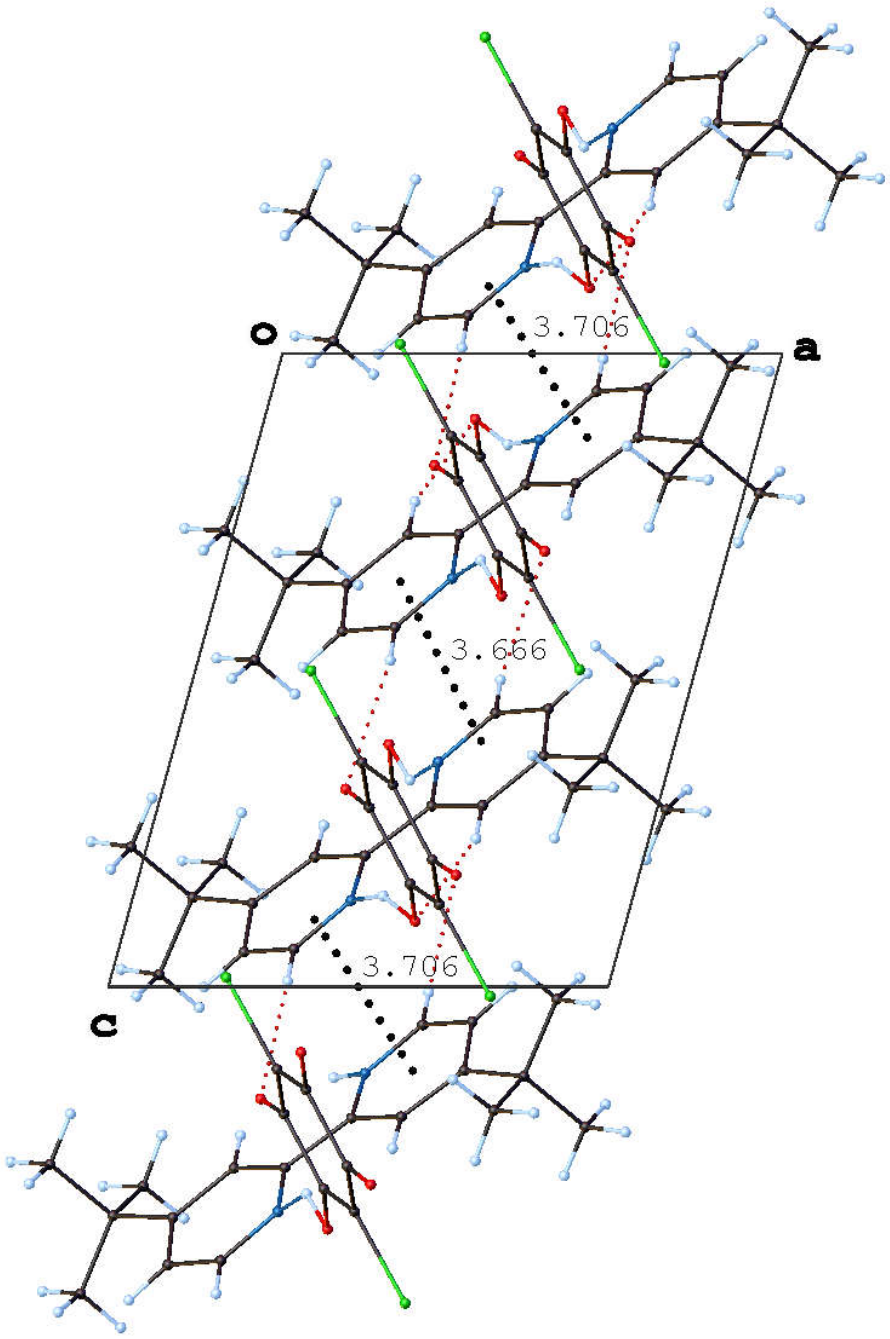

Fig. 4S. The interactions of the π-π stacking type in the crystal structure of the **dtBBP·BRA** complex at 155 K, the projection along ***b***-axis.

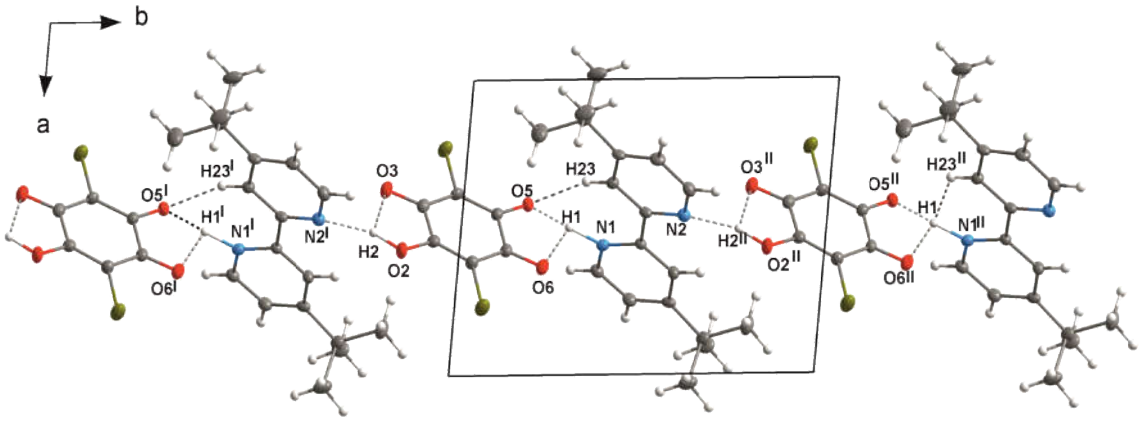

Fig. 5S. The ···dtBBP-IA-dtBBP-IA··· chain along the ***b***-axis.

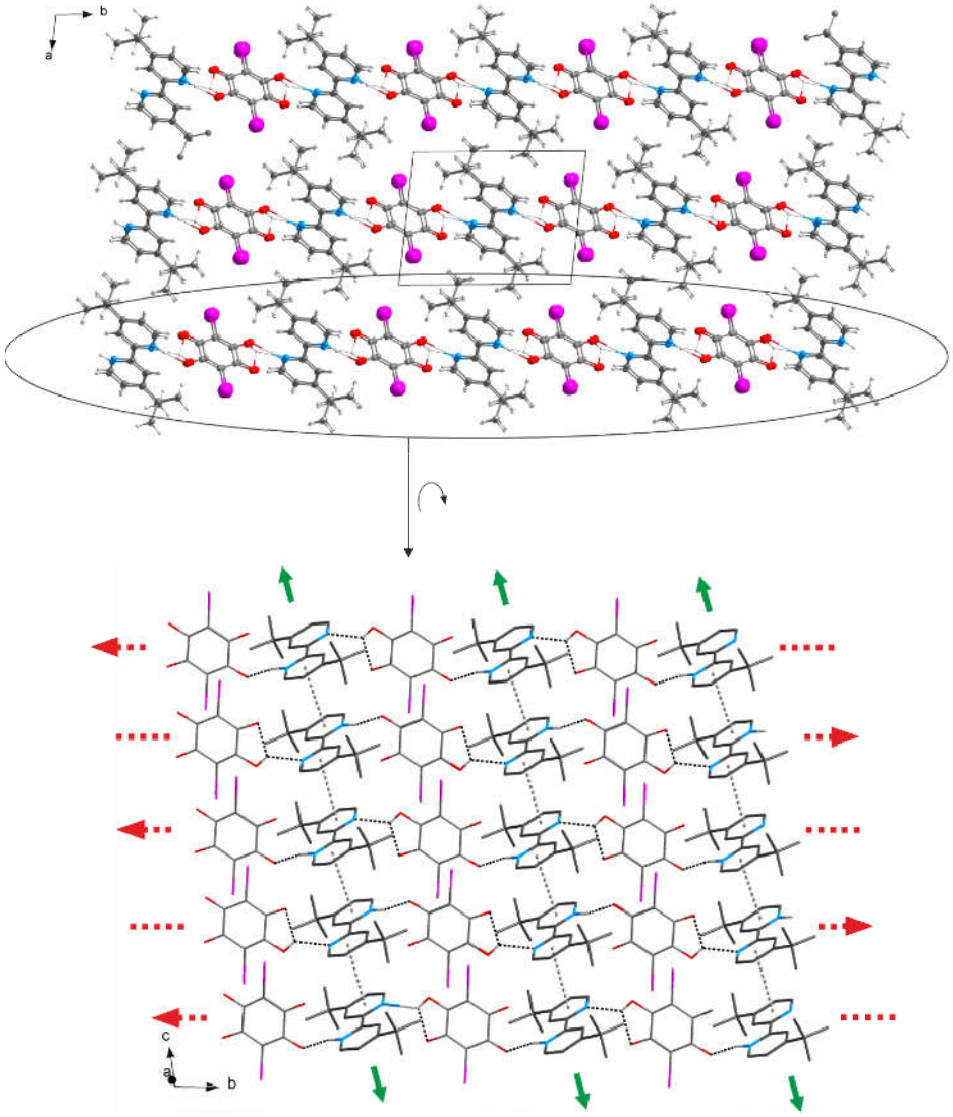

Fig. 6S. The layers and stacks of molecules in the structure of dtBBP·IA with the directions of the chains indicated (phase II).

a)

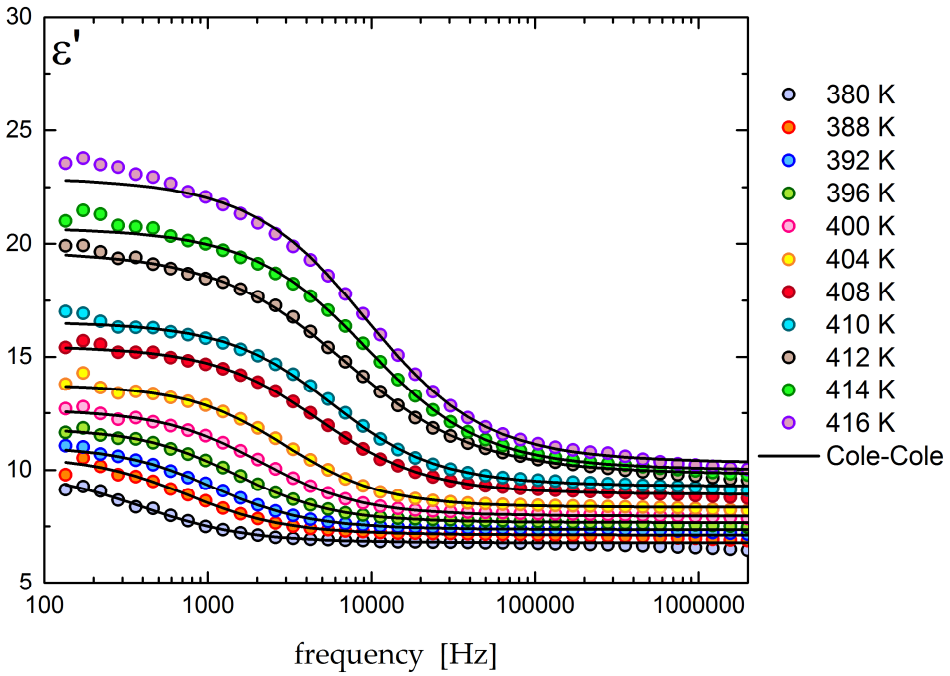

b)

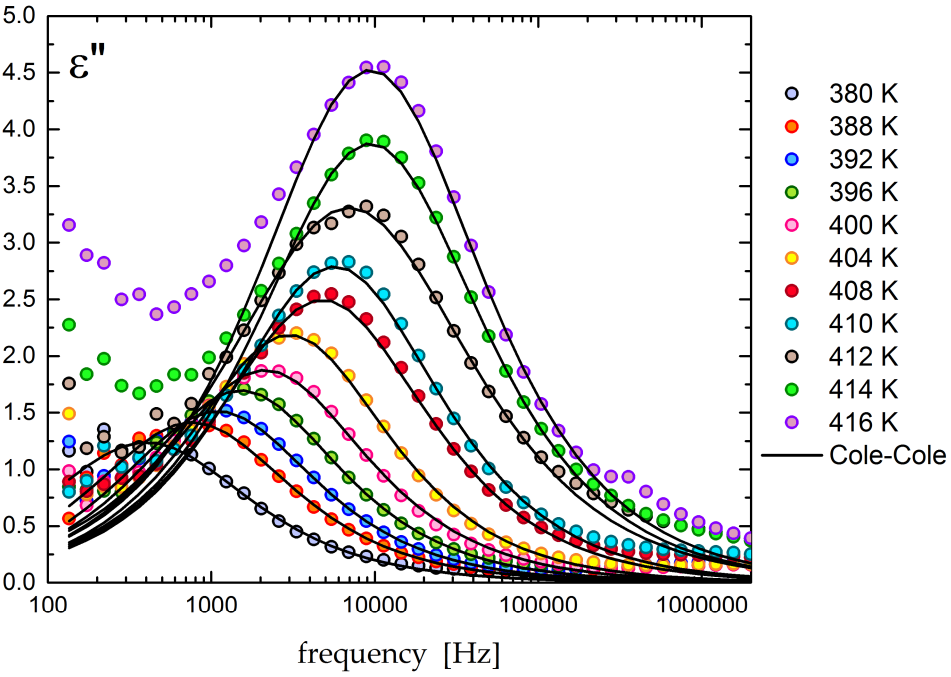

Fig. 7S. The frequency dependence of (a) the real part, ε': and (b) the imaginary part, ε"; of the permittivity at several temperatures measured for **dtBBP·BRA**.

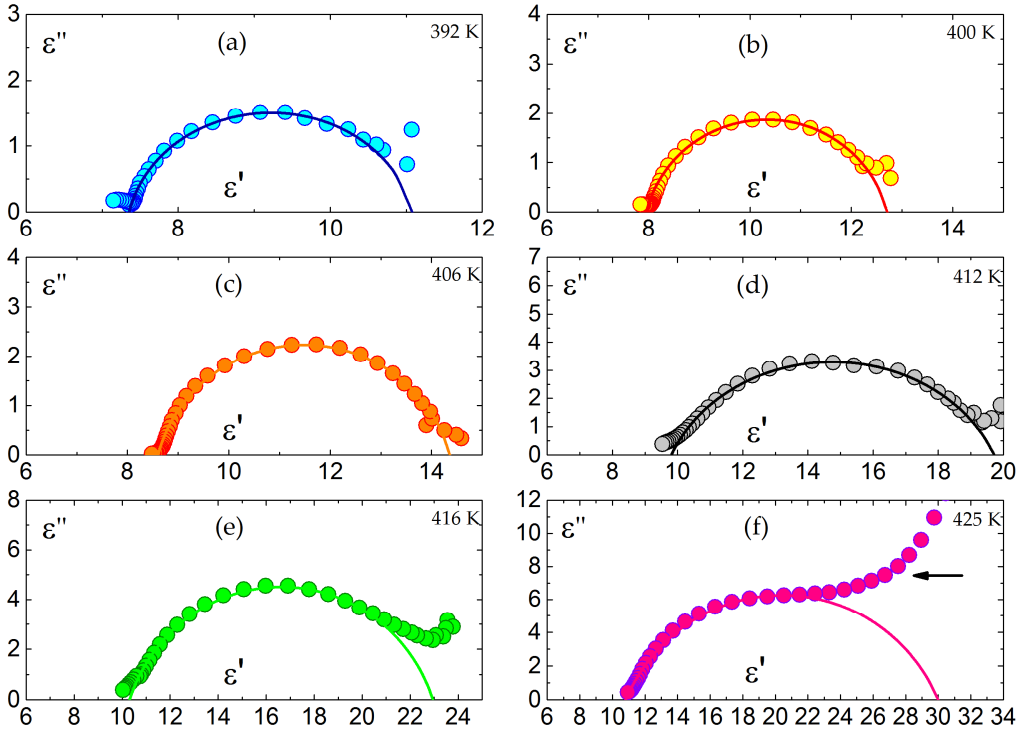

Fig. 8S. The dependence of ε" *versus* ε' for the single crystal of the dtBBP·BRA complex. The solid line represents fit to the Cole-Cole equation (Eq. (1)).

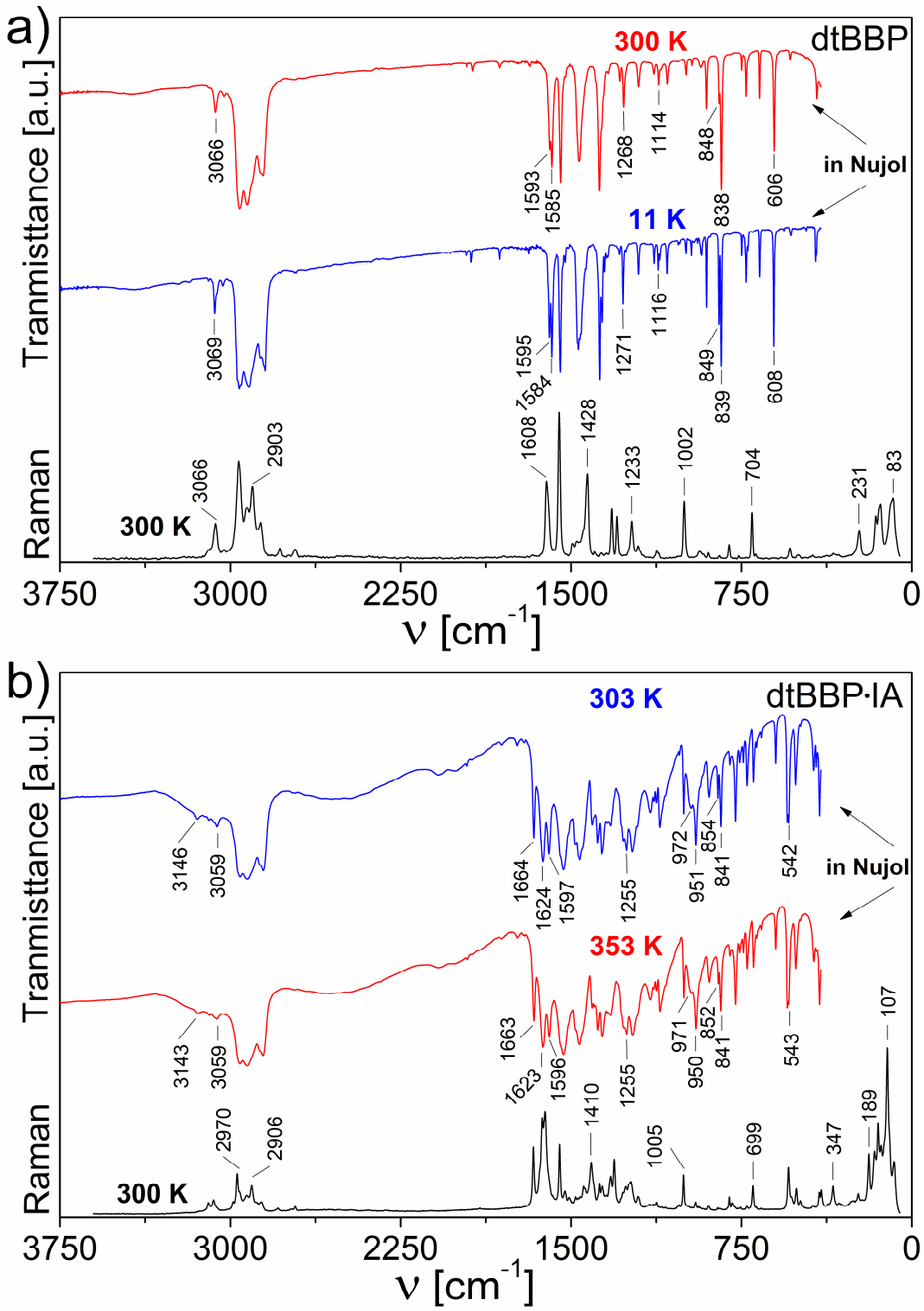

Fig. 9S. Raman and IR spectra of the a) pure-**dtBBP** and b) **dtBBP·IA**

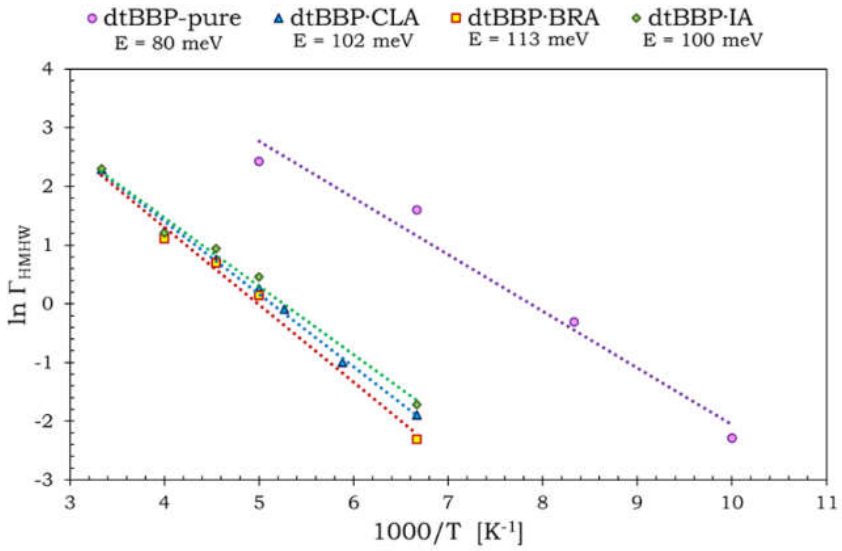

Fig. 10S. Temperature dependence of the average value lnΓ versus 1000/T for the pure **dtBBP** base (violet-circle), **dtBBP·CLA** (blue-triangle), **dtBBP·BRA** (yellow-square) and **dtBBP·IA** (green-diamond).

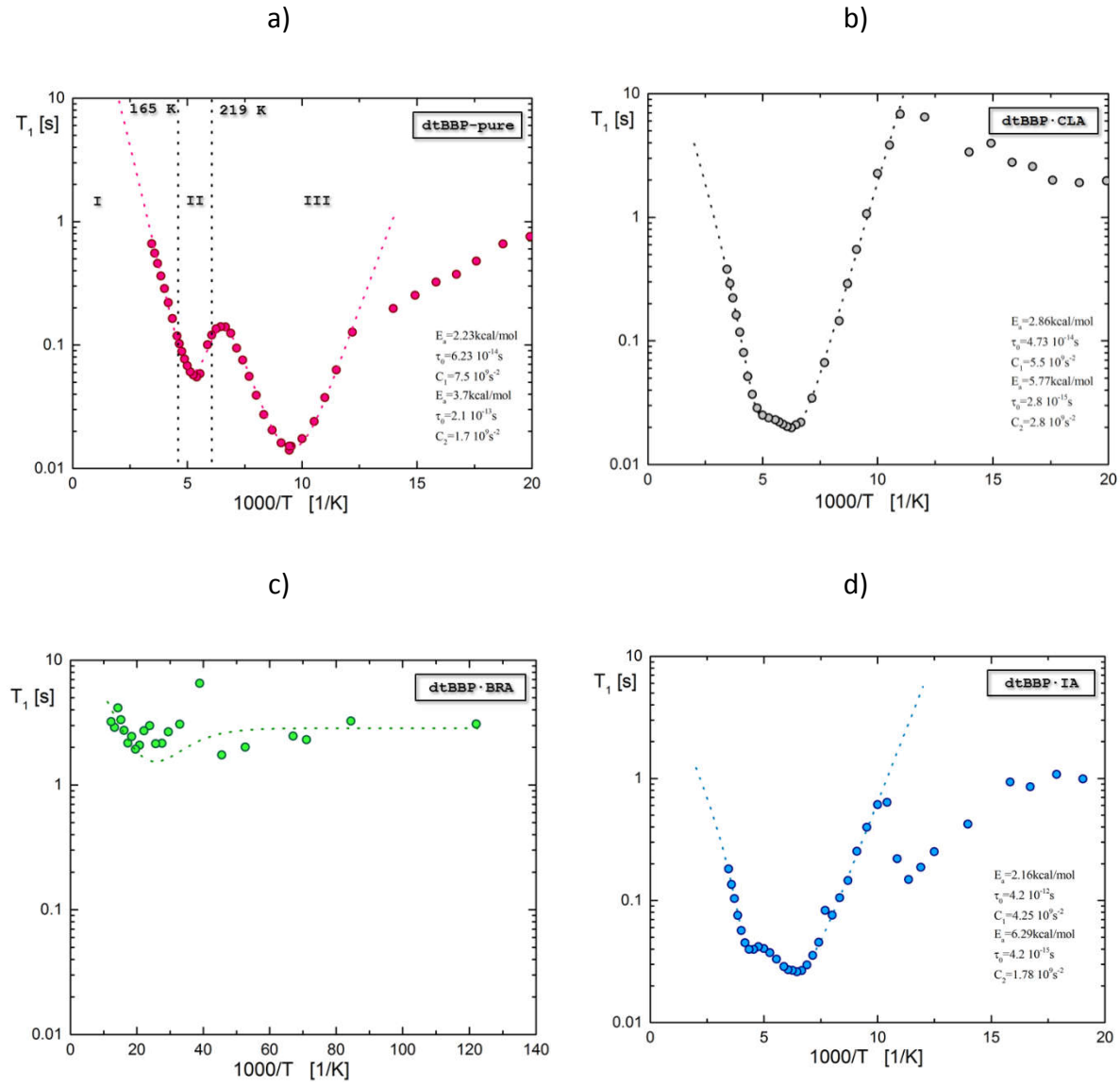

Fig. 11S. The temperature dependence of the spin–lattice relaxation time (T_1) for all complexes in the range between 8 and 100K a) pure-**dtBBP**, b) **dtBBP·CLA**, c) **dtBBP·BRA**, d) **dtBBP·IA**. The figures c, d, e and f were drawn for the temperature range between 100 and 50K.

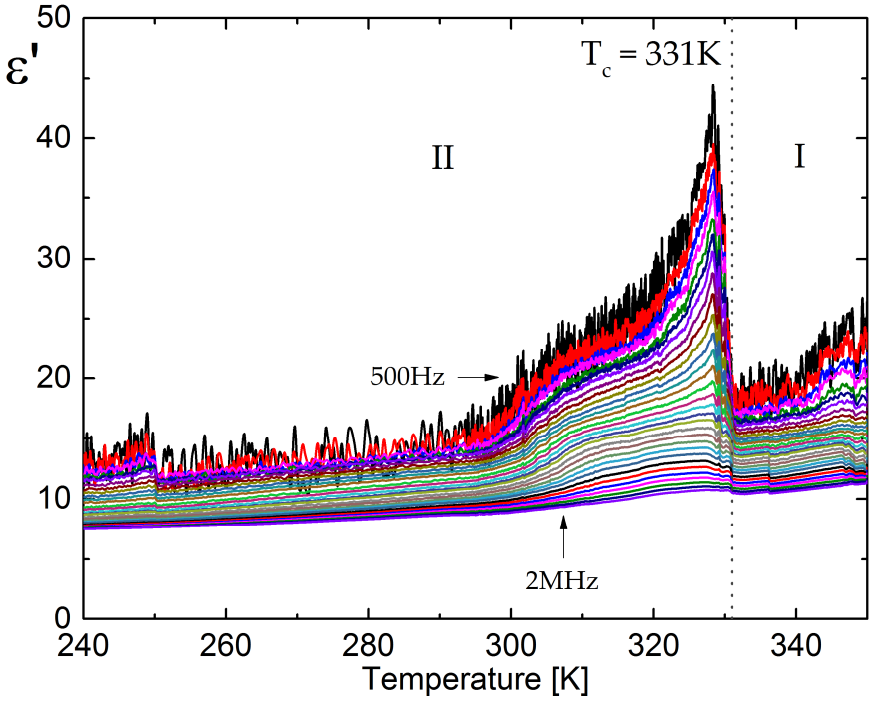

Fig. 12S. Temperature dependence of the real part of the complex electric permittivity for the as-grown **dtBBP· IA** single crystal.

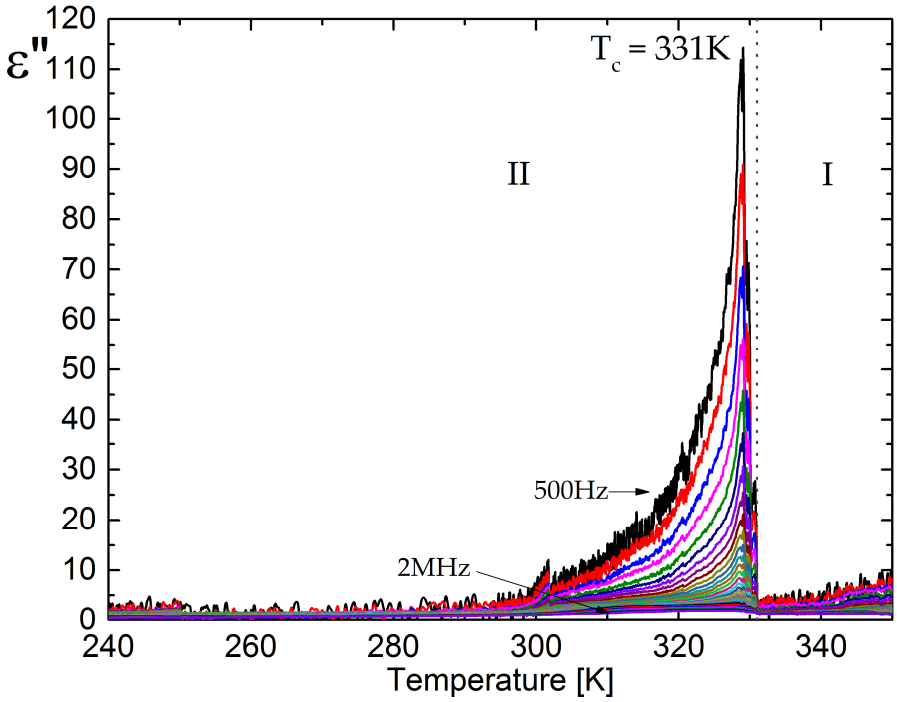

Fig. 13S. Temperature dependence of the imaginary part of the complex electric permittivity for the as-grown **dtBBP·IA** single crystal.

Table S1. Geometrical parameters (length and angle) and energies of the hydrogen bonds [1,2].

Geometrical parameters (length and angle) and energies of the hydrogen bonds	Conventional hydrogen bonds O-H···O, N-H···N		Unconventional hydrogen bonds C-H···X
	strong	weak	
Length A···B [Å]	2.2 – 3.0	3.0 – 4.0	2.7 – 3.0
Angle A···B [^{o}]	130 – 180	90 – 180	130 – 180
Energies of the hydrogen bonds [kcal/mol]	15 – 40	5	od 0.5

[1] G. A. Jeffrey, An Introduction to Hydrogen Bonding, Oxford University Press, 1997, p.12
[2] G. Gilli, P. Gilli, The Nature of the Hydrogen Bond, International Union of Crystallography Monographs on Crystallography, Oxford Science, Publication, 2009, p.

Table 2S. Crystal data and structure refinement for pure **dtBBP** (I, II, III) and its complexes: **dtBBP·BRA** (I) and **dtBBP·IA** (I, II).

Crystal: (phase)	**dtBBP (I)**	**dtBBP (II)**	**dtBBP (III)**	**dtBBP·BRA (I)**	**dtBBP·IA (I)**	**dtBBP·IA (II)**
Formula	$C_{18}H_{24}N_2$			$C_{24}H_{26}Br_2N_2O_4$	$C_{24}H_{26}I_2N_2O_4$	
T (K)	250(2)	190(2)	130(2)	155(2)	345(2)	295(2)
Crystal system	Monoclinic			Triclinic	Triclinic	
Space group	$P2_1/c$			$P\bar{1}$	$P\bar{1}$	
a (Å)	10.344(3)	10.316(3)	10.268(3)	8.951(3)	9.832(2)	9.261(3)
b (Å)	6.586(3)	6.334(3)	6.280(2)	11.491(5)	11.793(3)	11.779(3)
c (Å)	12.319(4)	24.559(4)	24.551(5)	11.910(3)	12.053(3)	11.997(4)
α (°)	90	90	90	98.84(3)	80.595(6)	99.09(4)
β (°)	102.04(5)	99.77(3)	99.49(3)	104.58(6)	66.706(6)	103.48(5)
γ (°)	90	90	90	93.42(4)	79.529(4)	94.58(4)
V (Å^3)	820.88(8)	1581.42(14)	1561.5(2)	1165.3(8)	1255.83(16)	1247.3(7)
Z	2	4	4	2	2	2
2θ Range (°)	3.382 to 28.708	3.325 to 28.783	2.827 to 30.77	3.093 to 36.830	2.683 to 30.865	2.707 to 30.164
ρ_{calc} (g cm^{-3})	1.239	1.122	1.142	1.614	1.746	1.758
Index ranges	-16<=h<=10 -8 <=k<=8 -12<=l<=12	-13<=h<=11 -8 <=k<=8 -33<=l<=32	-13<=h<=13 -8 <=k<=6 -23<=l<=34	-14<=h<=15 -17<=k<=14 -15<=l<=19	-12<=h<=12 -17<=k<=16 -11<=l<=17	-12<=h<=12 -7 <=k<=16 -16<=l<=16
μ(Mo K$_\alpha$) (mm^{-1})	0.063	0.063	0.067	3.512	2.536	2.553
F(000)	292	584	584	572	644	644
Crystal size [mm^3]	0.214 x 0.145 x 0.211	0.214 x 0.145 x 0.211	0.214 x 0.145 x 0.211	0.400 x 0.220 x 0.160	0.320 x 0.140 x 0.110	0.280 x 0.160 x 0.120
Reflections collected	4348	9886	7630	17495	10416	9785
Independent reflections	1886	3847	4273	8710	6397	6360
Completeness	to theta = 27.000 98.3%	to theta = 27.000 99.2%	to theta = 27.000 97.6%	to theta = 25.242 99.8 %	to theta = 27.000 93.1 %	to theta = 25.500 98.6 %
Refinement method	Full-matrix least-squares on F2					
Data / restraints /	1886 / 0 / 119	3847 / 0 / 235	4273 / 0 / 187	8710 / 0 / 297	6397 / 0 / 316	6360 / 0 / 316
Goodness-of-fit on F^2	1.122	1.033	1.036	0.912	1.013	1.044
Final R indices [I>2sigma(I)]	R1 = 0.0721, wR2 = 0.1843	R1 = 0.0671, wR2 = 0.1712	R1 = 0.0681, wR2 = 0.1514	R1 = 0.0685, wR2 = 0.1624	R1 = 0.0353, wR2 = 0.0785	R1 = 0.0299, wR2 = 0.0676
R indices (all data)	R1 = 0.1323, wR2 = 0.220	R1 = 0.1146, wR2 = 0.1902	R1 = 0.1171, wR2 = 0.1850	R1 = 0.1129, wR2 = 0.1754	R1 = 0.0699, wR2 = 0.0952	R1 = 0.0438, wR2 = 0.0747
Largest diff. peak and hole [eÅ^3]	0.332 and -0.286	0.236 and -0.277	0.381 and -0.238	1.056 and -1.714	0.335 and -0.342	0.395 and -0.473

Table 3S. Selected bond lengths [Å] and angles [º] for **dtBBP** at 130 **(III)**, 190 **(II)** and 250 K **(I)**.

[Å, º]	**dtBBP (III)**	**dtBBP (II)**	**dtBBP (I)**
4,4'-dtBBP			
N(1)-C(12)	1.343(2)	1.343(2)	1.349(2)
N(1)-C(16)	1.337(2)	1.334(2)	1.330(2)
N(2)-C(21)	1.342(2)	1.337(2)	-
N(2)-C(61)	1.341(2)	1.341(2)	-
C(12)-C(21)	1.490(2)	1.490(2)	1.507(2)
C(16)-N(1)-C(12)	116.63(16)	116.4(2)	115.8(2)
C(61)-N(2)-C(21)	116.88(16)	122.8(2)	-
N(1)-C(12)-C(13)	123.13(17)	122.94(2)	123.4(2)
N(1)-C(12)-C(21)	115.86(16)	116.1(2)	115.2(2)
N(1)-C(16)-C(15)	124.06(17)	124.7(1)	124.5(2)
N(2)-C(21)-C(12)	116.39(16)	116.2(2)	-
N(2)-C(21)-C(31)	122.65(17)	122.8(2)	-
N(2)-C(61)-C(51)	124.03(17)	123.9(2)	-
N(2)-C(21)-C(12) -N(1)	179.10(4)	179.7(2)	180

Table 4S. Selected bond lengths [Å] and angles [º] for **dtBBP·CLA** at 295[3], for **dtBBP·BRA** at 155 K and for **dtBBP·IA** at 295**(II)**, 345 K **(I)**.

[Å, º]	**dtBBP·CLA**	**dtBBP·BRA**	**dtBBP·IA (II)**	**dtBBP·IA (I)**
4,4'-dtBBPH$^+$				
N(1)-C(12)	1.358(2)	1.355(5)	1.347(1)	1.351(2)
N(1)-C(16)	1.350(2)	1.348(5)	1.344(1)	1.332(2)
N(2)-C(21)	1.353(2)	1.346(5)	1.346(1)	1.355(2)
N(2)-C(61)	1.342(2)	1.347(5)	1.335(1)	1.328(2)
C(12)-C(21)	1.494(2)	1.486(5)	1.495(1)	1.483(2)
C(16)-N(1)-C(12)	121.5(1)	122.0(3)	121.8(1)	121.1(1)
C(61)-N(2)-C(21)	116.7(1)	116.9(3)	116.5(1)	116.1(1)
N(1)-C(12)-C(13)	118.4(1)	118.2(3)	118.6(1)	118.2(1)
N(1)-C(12)-C(21)	118.9(1)	119.1(3)	119.5(1)	118.8(1)
N(1)-C(16)-C(15)	121.2(1)	120.3(4)	120.6(1)	122.1(1)
N(2)-C(21)-C(12)	114.6(1)	114.4(3)	114.4(1)	114.3(1)
N(2)-C(21)-C(31)	122.3(1)	123.2(3)	123.1(1)	122.4(1)
N(2)-C(61)-C(51)	124.3(1)	122.8(4)	123.7(1)	125.2(1)
N(2)-C(21)-C(12) -N(1)	177.75(4)	177.89(4)	178.8(1)	179.4(1)
XA$^-$				
X(1)-C(1)	1.732(3)	1.885(4)	2.102(3) 2.040	2.101(3) 2.032
X(2)-C(4)	1.732(3)	1.890(4)	2.108(3) 2.037	2.102(3) 2.027
O(2)-C(2)	1.329(2)	1.326(4)	1.331(2)	1.330(2)
O(3)-C(3)	1.242(2)	1.239(4)	1.239(2)	1.233(2)
O(5)-C(5)	1.265(2)	1.261(4)	1.260(2)	1.261(2)
O(6)-C(6)	1.230(2)	1.223(4)	1.221(2)	1.210(2)
C(1)-C(2)	1.352(2)	1.342(5)	1.353(2)	1.342(2)
C(2)-C(3)	1.514(2)	1.452(5)	1.510(2)	1.501(2)
C(3)-C(4)	1.422(2)	1.526(5)	1.413(2)	1.422(2)
C(4)-C(5)	1.397(2)	1.424(5)	1.394(2)	1.377(2)
C(5)-C(6)	1.540(2)	1.378(5)	1.541(2)	1.549(2)
C(1)-C(6)	1.458(2)	1.556(5)	1.461(2)	1.452(2)
C(1)-C(2)-C(3)	121.9(1)	122.0(3)	123.1(1)	123.2(1)
C(4)-C(3)-C(2)	118.0(1)	117.2(3)	117.7(1)	117.8(1)
C(4)-C(5)-C(6)	118.0(1)	117.7(3)	118.5(1)	118.5(1)
C(1)-C(6)-C(5)	118.8(1)	118.6(3)	118.8(1)	118.5(1)
O(2)-C(2)-C(1)	120.6(1)	122.8(3)	121.6(1)	121.8(1)
O(2)-C(2)-C(3)	116.5(1)	115.2(3)	115.3(1)	115.1(1)
O(3)-C(3)-C(2)	116.2(1)	115.7(3)	115.7(1)	116.2(1)
O(3)-C(3)-C(4)	125.8(1)	127.1(3)	126.6(1)	126.1(1)
O(5)-C(5)-C(4)	125.3(1)	125.7(3)	125.2(1)	125.3(1)
O(5)-C(5)-C(6)	116.8(1)	116.6(3)	116.3(1)	116.1(1)
O(6)-C(6)-C(1)	123.1(1)	124.4(3)	122.8(1)	123.4(1)
O(6)-C(6)-C(5)	118.1(1)	117.1(3)	118.4(1)	118.1(1)

X = Br, Cl, I

Table 5S. Hydrogen bonds in the crystalline state of **dtBBP·CLA** [Å,º].

D-H...A	d(D-H)	d(H...A)	d(D...A)	<(DHA)
N(1)-H(1)...O(5)	1.05(2)	1.60(2)	2.6139(17)	162(2)
N(1)-H(1)...O(6)	1.05(2)	2.38(2)	2.9526(16)	113.3(17)
O(2)-H(2)...O(3)	0.94(2)	2.17(2)	2.6563(17)	110.7(17)
O(2)-H(2)...N(2)#1	0.94(2)	1.88(2)	2.7343(17)	149(2)
C(13)-H(13)...O(3)#2	0.914(17)	2.934(15)	3.3686(19)	110.8(12)
C(31)-H(31)...O(5)	0.926(18)	2.474(18)	3.3405(19)	155.8(15)
C(16)-H(16)...O(3)#3	0.912(18)	2.363(18)	3.1471(19)	144.1(14)
C(72)-H(722)...O(3)#4	0.96	2.66	3.461(2)	141
C(74)-H(743)...O(5)#5	0.96	2.52	3.436(2)	160
C(76)-H(762)...O(6)#7	0.96	2.63	3.407(2)	138.1

#1 x,y-1,z #2 x,y+1,z #3 -x+1,-y,-z #4 x+1,y+1,z #5 -x+1,-y+1,-z #6 -x+1,-y+1,-z+1 #7 x-1,y,z

Table 6S. Hydrogen bonds in the crystalline state of **dtBBP·BRA** [Å,º].

D-H...A	d(D-H)	d(H...A)	d(D...A)	<(DHA)
N(1)-H(1)...O(5)	1.30(7)	1.39(7)	2.629(4)	156(6)
N(1)-H(1)...O(6)	1.30(7)	2.27(7)	2.972(4)	110(4)
O(2)-H(2)...O(3)	1.15(6)	1.99(6)	2.629(4)	111(4)
O(2)-H(2)...N(2)#1	1.15(6)	1.84(6)	2.758(4)	133(4)
C(13)-H(13)...O(3)#2	0.89(5)	3.11(4)	3.518(5)	110(3)
C(31)-H(31)...O(5)	0.96(5)	2.45(5)	3.332(5)	152(4)
C(16)-H(16)...O(3)#3	1.08(4)	2.17(4)	3.128(5)	147(3)
C(72)-H(722)...O(3)#4	0.96	2.55	3.456(5)	157.9
C(74)-H(743)...O(5)#5	0.96	2.48	3.421(5)	166.9
C(76)-H(762)...O(6)#7	0.96	2.52	3.400(4)	152.3

#1 x,y-1,z #2 x,y+1,z #3 -x+1,-y,-z #4 x+1,y+1,z #5 -x+1,-y+1,-z #6 -x+1,-y+1,-z+1 #7 x-1,y,z

[3] G. Bator, W. Sawka-Dobrowolska, L. Sobczyk, M. Owczarek, A. Pawlukojć, E. Grech and J. Nowicka-Scheibe, *Chem. Phys.*, 2012, **392**, 114–121.

Table 7S. Hydrogen bonds in the crystalline state of **dtBBP·IA** at 345K **(I)** and 295K **(II)** [Å,º].

D-H...A	d(D-H)	d(H...A)	d(D...A)	<(DHA)
345 K **(I-phase)**				
N(1)-H(1)...O(5)	0.931(2)	1.719(2)	2.622(2)	162.2(2)
N(1)-H(1)...O(6)	0.931(2)	2.509(2)	3.032(2)	115.8(2)
O(2)-H(2)...O(3)	0.868(2)	2.149(2)	2.611(2)	112.7(2)
O(2)-H(2)...N(2)#1	0.868(2)	2.114(2)	2.843(2)	141.2(2)
295 K **(II-phase)**				
N(1)-H(1)...O(5)	0.950(2)	1.713(2)	2.637(2)	163.3(2)
N(1)-H(1)...O(6)	0.950(2)	2.510(2)	3.023(2)	114.1(2)
O(2)-H(2)...O(3)	0.914(2)	2.042(2)	2.617(2)	119.6(2)
O(2)-H(2)...N(2)#1	0.914(2)	2.113(2)	2.482(2)	134.0(2)

#1 x,y-1,z

Table 8S. Wavenumber (cm^{-1}), intensity and tentative assignments of the bands observed in the IR and Raman spectra of **dtBBP** at 11 and 300 K.

dtBBP			
IR in Nujol		FT-Raman	TENTATIVE ASSIGMENT
T = 11 K	T = 300 K	T = 300 K	
3419 vw	3428 vw		ν_{as}(O H)
3224 vw			
3179 vw	3185 vw		ν_{s}(O H)
3096 vw	3093 vw	3100 vw	ν(CH)
3082 vw			
3069 w	3066 w	3066 w	
3057 vw sh			
		3048 vw	
3033 vw		3038 vw	
	3028 vw	3027 vw	
3006 vw			
		2963 s	$\nu_{as}(CH_3)$
		2927 w	$\nu_{s}(CH_3)$ + CH_3 as. def.
		2903 m	
		2867w	$\nu_{s}(CH_3)$
2779 vw	2781 vw	2781 vw	
		2746 vw	
		2740 vw	
2718 vw	2718 vw	2714 vw	
2711 vw			
	2684 vw		
2669 vw			
2632 vw			
2591 vw	2596 vw		
2563 vw			
2554 vw	2559 vw		
2517 vw			
2506 vw	2510 vw		
2381 vw	2386 vw		
2348 vw	2348 vw		
2311 vw	2304 vw		
2291 vw			
	2235 vw		
2031 vw	2029 vw		
1961 vw	1959 vw		
1940 vw	1933 vw		

1815 vw	1814 vw		
	1734 vw		
1685 vw	1685 vw		
	1682 vw		
		1608 m	
1595 s	1593 s	1598 w	i.p. ring
1584 vs	1585 s		
		1578 vw	
1567 vw	1566 vw		
1560 vw	1560 vw		
1547 vs	1546 vs	1552 vs	ν_{as}(N C)
1534 vw sh			
1525 vw	1523 vw		
1518 vw		1519 vw	
1513 vw	1508 vw		
1501 vw	1501 vw		
1491 vw	1492 vw	1493 vw	
1472 s sh		1475 vw	
1467 s N	1464 s N		
1461 s			$\delta(CH_3)$
1455 s			
1449 m sh		1446 vw	
1434 vw			
1421 vw	1421 vw	1428 m	
1416 vw			
1392 vw	1391 vw sh	1396 vw	
1374 vs	1375vs		
1366 m sh	1365 m sh	1366 vw	$\delta_s(CH_3)$
1363 s			
1353 w	1355 w sh		
1343 vw		1343 vw	
1337 vw	1336 vw		
		1321 w	
1309 vw			
1295 vw		1298 w	
1287 vw	1285 vw		
1271 m	1268 w		
1259 vw			
1240 vw			
1232 vw		1233 w	i.p. ring
1203 w	1203 w	1204 vw	δ(CH) + ν_s(N C)
1192 vw			

1183 vw			
1169 vw	1168 vw		
1152 vw			
1144 vw			
1134 w	1135 vw		
		1122 vw	
1116 w	1114 w	1115 vw	$\rho(CH_3)$
1109 w	1105 vw		$\rho(CH_3) + \delta$(ring)
1094 vw			
1077 w	1076 w		
1059 vw			
1029 vw	1031 vw		
1022 vw			
1002 vw		1002 w	
994 vw	994 vw		
979 vw			
970 vw	968 vw		
958 vw			
		951 vw	$\rho(CH_3)$
943 vw			
		934 vw	$\rho(CH_3)$
928 vw	929 vw		
925 vw			
918 vw		918 vw	$\rho(CH_3)$
903 m	904 m		o.p. CH
896 vw		896 vw	
890 vw			
849 m	848 w	847 vw	
839 vs	838 vs		i.p. ring
819 vw			
803 vw	798 vw	804 vw	δ(ring)
		762 vw	
749 w N	749 vw N		τ(ring)
739 vw	739 vw		o.p. CH
730 m N	730 w N		
722 vw			
700 vw		704 w	
688 vw		687 vw	
670 w	671 w		
608 vs	606 s		o.p. ring
589 vw	589 vw		
562 vw			

536 vw sh	535 vw	536 vw	τ(ring)
532 vw			
		505 vw	
465 vw	469 vw	496 vw	
		450 vw	δ(CCN)
435 vw		437 vw	o.p. ring
424 w			
420 w	418 w		
409 vw		408 vw	δ(ring)
		388 vw	
		374 vw	
		359 vw	o.p. ring
		345 vw	
		322 vw	
		231 vw	τ(CCNC) + (CH) + o.p ring
		158 w	
		145 w	
		138 w	
		92 w	
		83 w	

[a] s: strong, m: medium, w: weak, vw: very weak, sh: shoulder, s: symmetric, as: asymmetric, N: Nujol, i.p. in plane, o.p. out of plane, str. streching, def. deformation.

Table 9S. Wavenumber (cm^{-1}), intensity and tentative assignments of the bands observed in the IR and Raman spectra of **dtBBP·IA** at 303 **(II)** and 353 K **(I)**.

dtBBP·IA			
IR in Nujol		FT-Raman	TENTATIVE ASSIGMENT
T = 303 K	T = 353 K	T = 300 K	
3500 vw	3502 vw		ν_{as}(O H)
3309 vw	3309 vw		ν(N H)
3207 w	3209 w		ν_{s}(O H)
3146 w	3143 w		ν(CH)
3113 w	3111 w		
3095 w	3093 w	3095 vw	ν(CH)
3071 m sh	3072 m sh	3073 vw	
3059 m	3059 m		
		2987 vw	
		2970 w	$\nu_{as}(CH_3)$
		2958 vw sh	
		2935 vw	
		2926 vw	$\nu_{as}(CH_3) + \delta_{as}(CH_3)$
		2906 vw	
		2882 vw	
		2862 vw	$\nu_{s}(CH_3)$
		2789 vw	
		2732 vw	
2722 w	2715 w	2714 vw	
2669 w	2672 w		
2606 w	2601 w		
2555 w			
2522 w	2522 w		
2470 w	2467 w		
2389 w	2391 w		
	2342 w		
2084 w	2084 w		
2008 w	2012 w		
1959 w	1956 w		
1936 vw	1934 vw		
1831 vw	1828 vw		
1806 vw	1806 vw		
1737 vw	1737 vw		
1706 vw	1709 vw		
	1703 vw		
1664 s	1663 s	1665 m	

		1639 w sh	
1624 vs	1623 vs	1626 m	ν(C=C) + δ(OH···N)
		1613 s	
1597 vs	1596 vs	1598 w sh	i.p. ring
1580 m	1579 m	1581 vw	
1547 vs sh	1548 vs sh	1550 m	ν_{as}(N C)
1533 vs	1533 vs	1526 vw	
1509 s sh	1508 s sh	1507 vw	
1497 s	1497 s		
1482 s	1483 vs sh	1480 vw	
1478 s	1477 vs sh		δ(CH_3) + ν_{as}(N C)
1468 vs sh	1466 vs sh	1469 vw	
1462 vs	1462 vs	1460 vw	δ(CH_3) + ν(C C)
1448 s sh	1446 vs sh	1444 vw	
		1437 vw	
1406 s	1406 s	1410 w	δ(CH_3) + ν_s(N C)
1396 s sh	1397 s	1398 vw sh	
1383 vs	1382 vs	1381 vw sh	δ(CH_3)
		1374 vw	δ(CH_3) + δ(OH···N)
1364 vs	1363 vs	1363 vw	δ(OH···N) + ν(C O) + ν_s(C C)
1341 s	1340 s	1342 vw	
1325 s	1325 s	1324 w	
1317 s sh	1316 s sh		
1309 m sh	1309 m sh	1310 w	
1296 m	1296 m		δ(CNC) + ν(C CH_3) + δ(CH_3)
1279 s	1278 s sh	1282 vw sh	
1270 vs	1268 vs	1272 vw	δ(NC) + (OH···N)
1255 vs	1255 vs	1259 vw	
		1246 vw sh	
1230 vs	1229 vs	1237 vw	δ(OH···N) + ν(C C) + i.p. ring
1208 s	1206 s	1205 vw	δ(OH···N) + ν_s(N C)
		1199 vw sh	
1151 s	1151 s	1154 vw	
		1148 vw	
1135 m	1135 m	1136 vw	
1124 m	1123 m	1123 vw	
1109 s	1108 s	1111 vw	
1097 sh s	1097 sh s	1098 vw	
1082 m sh	1081 s	1084 vw	
1030 w	1030 w	1031 vw	
1024 w	1023 w	1024 vw	
1004 s	1004 s	1005 w	ρ(CH_3) + (OH···N) + δ(ring)

		980 vw	
972 s	971 s		ν_{as}(C=C) + δ(OH···N)
951 vs	950 vs	952 vw	ρ(CH_3)
		940 vw	ρ(CH_3) + (OH···N) + ν_{as}(C=C)
930 m	930 m	932 vw	
916 m	917 m		
893 m	892 m	895 vw	
854 m	852 m	854 vw	
841 vs	841 s	846 vw	
		813 vw sh	
801 w	801 w	804 vw	δ(ring) + δ(OH···N)
		791 vw	
		787 vw sh	
776 s	776 s	778 vw	IA
		765 vw	
758 w	758 w	760 vw	δ(C I)
751 w sh	749 w sh	753 vw	τ(ring)
742 w	741 w		
726 m	725 m	727 vw	
697 m	697 m	699 vw	
683 w	683 w	682 vw	
662 vw	662 vw	663 vw	
599 w	599 w		
548 vs	548 vs		τ(ring)
542 vs	543 vs	542 w	τ(ring)
		530 vw sh	
512 vs	511 m	507 vw	
489 vw	489 vw	489 vw	τ(ring)
		478 vw	
432 m	431 m		o.p. ring
421 m	419 w		
406 vs	406 vs	407 vw	δ(C=C=C) + δ(ring)
		398 vw	
		368 vw	
		356 vw sh	ν(H···O) + δ(CCO)
		347 vw	o.p. ring
		319 vw	
		310 vw sh	ν(C I) + δ(C=C=O) + δ(C=C O)
		268 vw sh	
		258 vw	
		253 vw sh	
		246 vw sh	

		235 vw	τ(CCNC) + (CH) + o.p ring
		218 vw	
		189 w	ν(I···I)
		164 m	
		149 m	(C O)
		134 m	(C=O) + (C O)
		121 m sh	
		107 vs	
		97 m sh	
		77 w	

[a] s: strong, m: medium, w: weak, vw: very weak, sh: shoulder, s: symmetric, as: asymmetric, N: Nujol, i.p. in plane, o.p. out of plane, str. streching, def. deformation.

Table 10S. Parameters, E_a, τ_0, C obtained from ^{1}H-NMR interaction.

	Acids		**pure-dtBBP**		**dtBBP-CLA**		**dtBBP-BRA**	**dtBBP-IA**	
parameter	**CLA**	**BRA**	**min I**	**min II**	**min I**	**min II**	**min I**	**min I**	**min II**
E_a [kJ/mol]	3.2	1.2	9.3	15.5	12.0	24.1	1.2	9.0	26.3
τ_0 [s]	$1.1\ 10^{-11}$	$1.3\ 10^{-10}$	$6.2\ 10^{-14}$	$2.1\ 10^{-13}$	$4.7\ 10^{-14}$	$2.8\ 10^{-15}$	$1.3\ 10^{-10}$	$4.2\ 10^{-12}$	$4.2\ 10^{-15}$
C [s^{-2}]	$2.8\ 10^{6}$	$1.2\ 10^{7}$	$7.5\ 10^{9}$	$1.7\ 10^{9}$	$5.5\ 10^{9}$	$2.8\ 10^{9}$	$4.2\ 10^{7}$	$1.8\ 10^{9}$	$4.3\ 10^{9}$